THE ROYAL SOCIETY

doi 10.1098/rspb.2001.1635

The avian tail reduces body parasite drag by controlling flow separation and vortex shedding

W. J. Maybury[1]† and J. M. V. Rayner[2*]

[1]*School of Biological Sciences, University of Bristol, Woodland Road, Bristol BS8 1UG, UK*
[2]*School of Biology, University of Leeds, Clarendon Way, Leeds LS2 9JT, UK*

The aerodynamic effect of the furled avian tail on the parasite drag of a bird's body was investigated on mounted, frozen European starling *Sturnus vulgaris* in a wind tunnel at flight speeds between 6 and 14 m s^{-1}. Removal of tail rectrices and dorsal and ventral covert feathers at the base of the tail increased the total parasite drag of the body and tail by between 25 and 55%. Flow visualization and measurements of dynamic pressure in the tail boundary layer showed that in the intact bird a separation bubble forms on the ventral side of the body, and reattaches to the ventral side of the tail. This bubble is a consequence of the morphology of the body, with a rapid contraction posterior to the pelvis and hind legs. The tail and the covert feathers at its base act as a combined splitter plate and wedge to control vortex shedding and body wake development, and thereby are important to minimize drag. This hitherto unsuspected mechanism is central to understanding the morphology of the avian body, and may have had a significant influence on the evolution of avian tail morphology by pre-adapting the tail for radiation and specialization as an aerodynamic lifting structure and as an organ of communication in sexual selection.

Keywords: bird; starling; flight; tail; drag; aerodynamics

1. INTRODUCTION

The functions of the avian tail have been widely and hotly debated. Aerodynamically the tail is a means of directional control and stability, and it can form a supplementary lifting surface enhancing lift generation in slow flight (e.g. Von Holst & Küchemann 1941; Pennycuick 1975; Norberg 1990; Thomas 1993, Norberg 1994). The combination of tail and wings may be beneficial, with the tail possibly acting as a drag-reducing flap which interacts with vortices in the wake of the wings to reduce induced drag (Hummel 1991, 1992; Thomas 1996*a*). As a balancing and lifting surface, a long tail played a key role in early avian evolution (Peters & Gutmann 1985; Gatesy & Dial 1996), but subsequently the bird tail rapidly reduced in size and took on different aerodynamic significance (Rayner 2001; Rayner *et al*. 2001). While a biomechanical function of the tail is not disputed, others argue that the tail is more important in communication and sexual selection, citing examples from birds with elongated tails (e.g. Evans *et al*. 1994) or from species with streamers on the outermost tail rectrices (e.g. barn swallows) in which tail design is supposed to be aerodynamically suboptimal. The relative merits of aerodynamic and behavioural explanations for extreme tail morphologies are vigorously disputed (e.g. Norberg 1994; Evans & Thomas 1997; Møller *et al*. 1998; Barbosa & Møller 1999; Buchanan & Evans 2000). However, relatively few birds have such large tails (Fitzpatrick 1997, 1999), and in cruising flight in most birds the tail is furled to a narrow profile, so observations based on these exceptional cases may misrepresent the role of the tail in typical birds in normal flight.

*Author for correspondence (j.m.v.rayner@leeds.ac.uk).
†Present address: Westland Helicopters Limited, Box 231, Lysander Road, Yeovil, Somerset, BA20 2YB, UK.

The possibility that when furled the tail plays a significant aerodynamic role has not previously been considered. In this paper we combine measurements of body drag and boundary layer dynamic pressure with flow visualization observations to reveal that the furled tail plays a hitherto unsuspected, but important, aerodynamic rôle, reducing total body parasite drag in response to constraints of the avian Bauplan.

In lateral aspect, a bird's body lacks dorsoventral symmetry. The profile is approximately streamlined, but in species such as the starlings studied here the ventral outline reveals a bluff surface posterior to the pelvis and hind legs. In starlings, the tail when furled is relatively narrow compared to the breadth of the body, and covert feathers at the base of the tail create a smooth fairing between the body and tail. The bluff ventral profile leads us to expect the presence of a region of flow separation, at some airspeeds, and therefore of an unfavourably high magnitude of body drag. At the supercritical and transitional Reynolds numbers at which small birds fly (20 000 to 70 000), separation from a shape such as this is likely to be associated with dynamic vortex shedding. This suggests that regulation of boundary layer separation and vortex shedding could be a possible mechanism by which a bird reduces or controls drag.

Separation and vortex shedding are common phenomena of bluff bodies in air flows. A number of authors have shown that the wake structure of two-dimensional cylinders, bluff bodies and three-dimensional axisymmetrical bodies can be modified by placing a *splitter plate* on the wake centreline, downstream of the object (Degani 1991; Nakamura 1996; Anderson & Szewczyk 1997). Splitter plates reduce (or remove) the interaction between the shear layers formed on opposite sides of the object, in turn affecting the periodic vortex shedding process at the object's trailing edges (Anderson & Szewczyk 1997). By interfering with, and even preventing, vortex shedding, splitter plates narrow mean wake height, and can reduce

Received 3 November 2000 *Accepted* 19 February 2001

drag by up to 36% for cylinders at Reynolds numbers between 10^3 and 10^6 (Hoerner 1958), and by 50% for bluff bodies between Reynolds numbers 350 and 1150 (Mansingh & Oosthuizen 1990). By a similar mechanism, a wedge or fairing at the trailing edge of a bluff body can also control the motion of the shed vortices and can also reduce drag to a comparable extent (Hoerner 1958).

We hypothesize that—despite the body's lack of dorso-ventral or axial symmetry—the bird tail and the adjacent covert feathers act similarly to the splitter plate and/or wedge to form an important drag-reducing mechanism. The benefits from this mechanism exceed any additional drag due to the increased tail surface area exposed to the airflow.

2. MATERIAL AND METHODS

(a) *Experimental design*

Measurements were conducted on mounted specimens of European starling *Sturnus vulgaris* in an open circuit Eiffel-pattern wind tunnel with a closed working section 0.52 m × 0.52 m × 1.00 m in dimensions. Tunnel airspeeds used ranged from 6 to 14 m s^{-1} (Reynolds number of 22 000 to 50 000); over this speed range RMS turbulence in the centre of the working section around the bird was less than 0.35%. Birds were frozen with minimal disturbance to feather alignment; the wings were removed at the shoulder and the feet and legs at the knee joint, leaving a smooth-feathered body profile, and body feathers were treated with a light, even coating of hair wax (Pennycuick *et al.* 1988) so that feathers retained their position but some compliance remained in the integument. Body posture was determined from observation of video films of starlings flying in a wind tunnel made in the course of a different study (Ward *et al.* 1999). In steady horizontal flight the tail is held furled, so that the lateral sides of the most distal rectrices are close to parallel, and horizontal so that it generates little or no lift.

(b) *Drag measurements*

Birds were mounted on a sting passing laterally through the body close to the shoulder joint and the centre of mass of the body; wires concealed under the feathers maintained body and tail posture. Drag was measured from the deflection of strain gauges mounted on the sting (design following Bonser & Rayner 1996); strain gauge bridge output was collected through a commercial strain gauge amplifier (RS Components Ltd, Corby, UK) and digitized by a PC-based A/D converter (DAS 50, Keithly Instruments Inc., Cleveland, OH, USA) at a sampling rate of 300 Hz for 8190 readings per channel, and subsequently filtered and averaged. Drag measurements were highly repeatable in these and other similar experiments. Error bars shown for drag measurements are ± standard deviation of callibration error.

Because the starling body is relatively small compared to the wind tunnel cross-section, and because these experiments concentrate on drag and not lift, it was not necessary to apply blockage or other wind tunnel corrections. We corrected for sting drag and interference drag between the sting and the body by a protocol involving varying sting proportions and sting geometry, based on the methods of Rae & Pope (1984) and Tucker (1990).

Drag results are expressed in terms of the body drag coefficient, defined as

$$C_{\mathrm{D_b}} = D_\mathrm{b} / \tfrac{1}{2}\rho S_\mathrm{b} V^2, \qquad (1)$$

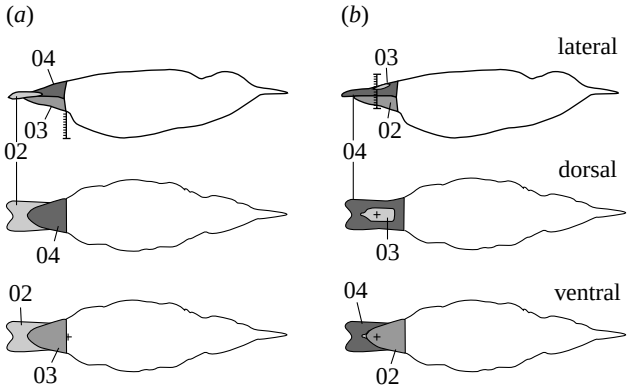

Figure 1. The experimental manipulation procedure, progressively removing segments of the tail. (*a*) Protocol 1 first eliminated the tail, and second the covert feathers. Protocol 2 (*b*) first prevented any function of the tail covert feathers, and then any effect of the tail in controlling ventral flow separation (see §§ 2 and 4). Steps 01 (before manipulations) and 04 (all tail and covert feathers removed) are the same for both experimental procedures. Also shown are the locations at which dynamic pressure was measured.

where S_b is the minimum frontal projected area of the body, and D_b is the body drag. Drag coefficient measurements are expressed in terms of Reynolds number (Re), defined in terms of air density ρ, air dynamic viscosity μ, airspeed V and a characteristic length of the object l (taken here to be the diameter of a circle equal in area to the frontal projected area S_b) as

$$\mathrm{Re} = \frac{\rho V l}{\mu}. \qquad (2)$$

Air density ρ was taken to be 1.225 kg m^{-3} and dynamic viscosity μ to be 1.82×10^{-5} kg m^{-1} s^{-1}, the values at sea level and 20 °C in the International Standard Atmosphere (Denny 1993).

(c) *Experimental manipulation of the tail*

Our hypothesis is that the tail, even when furled, has an effect on body drag that is much greater than can be explained by its shape alone. To test this, we measured drag for two starling bodies at a uniform angle of attack, while progressively manipulating the tail and the adjoining covert feathers to reduce tail size, according to two experimental protocols (figure 1). At each stage of tail reduction we measured drag at five speeds in the range of 6–14 m s^{-1}. The sequence of the manipulation varied between protocols, but the first and last steps (01, before manipulation, and 04 after removal of all tail rectrices and ventral covert feathers) were the same in each case. In protocol 1 the intermediate steps were first to cut off the rectrices protruding beyond the ventral covert feathers (step 02), then to remove the ventral covert feathers (03), and finally to remove the dorsal coverts and the remaining part of the rectrices (04). In protocol 2 the ventral covert feathers were removed first (02), then a mid-section of the rectrices was excised allowing pressure to equilibrate between dorsal and ventral surfaces of the tail (03), and finally the remaining parts of the rectrices were removed (04). The two protocols were designed to identify whether either or both of the tail and/or the feathers which form a fairing at the base of the tail affect the airflow over the body and have an effect on body drag, and if so to show whether the tail or the covert feathers is most important

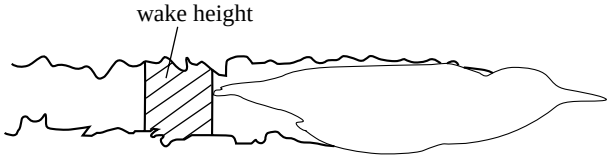

Figure 2. Sketch showing the wake height measured from flow visualization images of a starling as the average height over the area shown, extending a distance of 4 cm posterior to the position of the tip of the tail.

in controlling airflow. Previous flow visualization experiments (Maybury 2000) had shown that at most flight speeds in starlings (and other small birds) a laminar separation bubble forms ventrally beneath the base of the tail, and that it is important for minimizing body drag that this bubble reattaches to the distal ventral region of the tail; protocol 2 should enable identification of how this reattachment is controlled.

(d) *Dynamic pressure measurements*

We measured dynamic pressure in the boundary layer with a pitot-static tube purpose built from 1 mm diameter copper pipes attached to a Sen-I-Tran FCO 322, 0–100 Pa pressure transducer (Furness Controls Ltd, Bexhill-on-Sea, UK). Dynamic pressure q is determined from airspeed V and air density ρ as

$$q = \tfrac{1}{2}\rho V^2; \qquad (3)$$

to highlight the occurrence of separation, in which air tends to flow in the opposite direction to the free stream, we use the convention of giving negative values to dynamic pressure measurements to denote reverse flow.

(e) *Flow visualization*

We used the smoke-wire technique (Batill & Mueller 1981) to visualize airflow around the starling during steps 01, 02 and 04 of protocol 1, at airspeed 9 m s^{-1} (Re 35 000). A vertical nickel-chromium wire 0.05 mm in diameter (Ni90/Cr10 Goodfellow Cambridge Ltd, Huntingdon, UK), was stretched upstream across the flow field, and when coated with oil (Shell Ondina EL, Shell Oils, Manchester, UK) produced short bursts of smoke controlled electrically by resistive heating.

The flow field was illuminated in a vertical two-dimensional sheet by four Metz 45CL−3 flash guns synchronized with the heating pulse for the oil wire. Six photographs taken at each step were scanned (Nikon Coolscan, Nikon F3, Ilford XP5 black and white negative film, Nikon UK Ltd, Kingston upon Thames, UK); from the digitized photographs wake height was measured as an indirect estimate of drag (figure 2).

(f) *Data analysis*

Most statistical procedures and other data manipulations were undertaken in MS Excel 97. ANOVA were performed in Minitab 10.51Xtra (Minitab Inc. 1995), in all cases with the assumption of normal error distribution.

3. RESULTS

(a) *Drag*

In both protocols, each successive reduction in tail size had the effect of increasing drag coefficient, at all

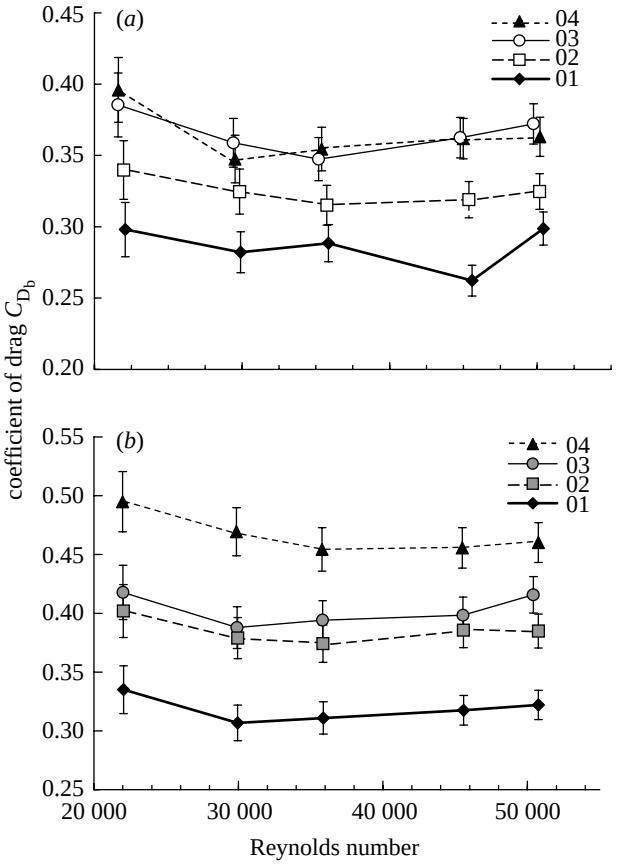

Figure 3. Drag coefficient (standard deviation error based on balance calibration) against Reynolds number, for starlings, according to (*a*) protocol 1 and (*b*) protocol 2, showing the effect of four progressive tail manipulations reducing tail size. The lowest and highest Reynolds numbers measured, based on length defined as mean diameter of body frontal area, are equivalent to airspeeds of 5.9 m s^{-1} and 13.5 m s^{-1}, respectively.

Reynolds numbers (and airspeeds) measured; the only exception was for the last two manipulations of protocol 1 where the difference in drag between 03 and 04 was indistinguishable (figure 3). In protocol 1 the first tail manipulation (01–02) removed the rectrices that extend beyond the ventral covert feathers; at a Reynolds number of 50 000 (13.5 m s^{-1}) this had the effect of increasing drag coefficient by 9%. The boundary layer was still able to reattach to the ventral coverts, and the point of reattachment only moved 2 mm downstream. At this stage the ventral outline still had a streamlined (or wedge-shaped) profile. Removal of the ventral coverts (steps 02–03) dramatically increased the drag coefficient (by a further 14% at a Reynolds number of 50 000). The boundary layer no longer reattached, and this explains why subsequent removal of the dorsal covert feathers (steps 03–04) did not further increase drag. The total increase in drag due to the removal of the tail and covert feathers was 25% at a Reynolds number of 50 000; at lower Reynolds numbers drag increased by between 17 and 38%.

In protocol 2 each successive tail manipulation had the effect of increasing drag coefficient. The first manipulation (01–02) removed the ventral covert feathers, which according to our hypothesis act as a wedge controlling detachment of the separation bubble from the ventral

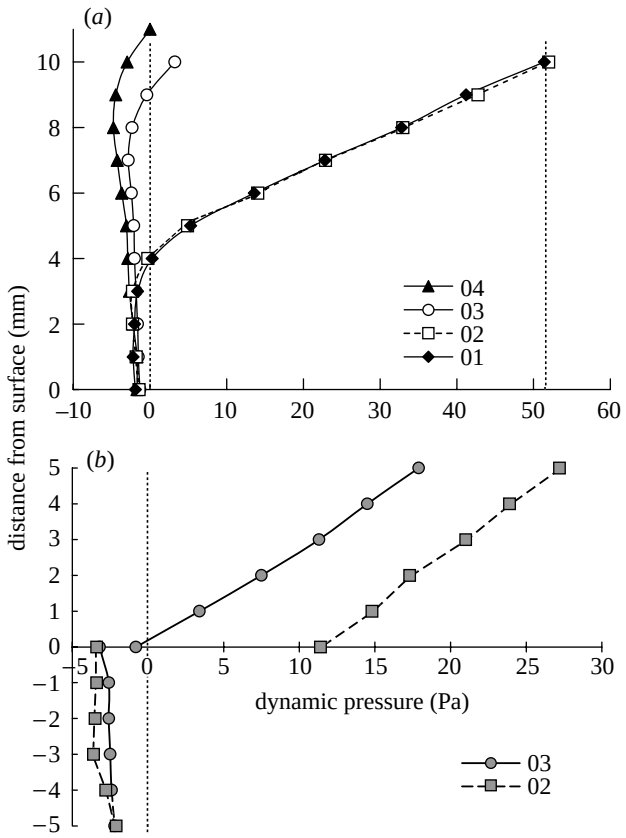

Figure 4. Dynamic pressure in the boundary layer, shown as negative to signify reverse flow in the separation bubble. A dynamic pressure of zero is usually accepted to be the point of separation (Young 1989). (*a*) During each step of protocol 1, measured on the ventral side of the tail at the root of the covert feathers, at sequential 1 mm intervals below the surface until a positive dynamic pressure was reached. Free stream airspeed 9.2 m s^{-1} corresponds to a dynamic pressure of 51.5 Pa. The size of the separation bubble increases markedly between steps 02 and 03. (*b*) During steps 02 and 03 of protocol 2, measured on the ventral (below axis) and dorsal (above axis) sides of the tail at the centre of the mid-section of the rectrices, to 5 mm above and below the surface at 1 mm intervals. The shallow linear increase in pressure with height shows that the dorsal boundary layer is thick and turbulent. Removal of the centre of the rectrices (step 03) induces weak separation on the dorsal side. At both steps, in the absence of the ventral coverts, the flow on the ventral side of the tail is still separated at this point.

side of the body. Removal of the ventral covert feathers increased the drag coefficient by 20% at a Reynolds number of 50 000. Removal of a middle section from the rectrices (02–03), which enabled the shear layers on the ventral and dorsal surfaces of the tail to interact and to equilibrate pressure, further increased drag coefficient by 8% at a Reynolds number of 50 000. The final treatment, removing the remaining rectrices (03–04), prevented the bubble from reattaching, and resulted in a corresponding increase in drag coefficient of 11% at a Reynolds number of 50 000. The total increase in drag coefficient due to the removal of the tail was 43% at a Reynolds number of 50 000; at lower Reynolds numbers the increase in drag ranged between 43 and 53%.

For both protocols the increase in drag with tail removal is sizeable and permanent, and cannot be compensated by other aerodynamic mechanisms. There are several possible explanations for the different magnitudes of the increase in drag coefficient between the two protocols: (i) the point of tail removal may have differed between specimens; (ii) there may have been differences in posture and differences in feather organization; and (iii) the birds may have differed in body size, shape and/or condition. These last two explanations were supported by the fact that the initial and final drag coefficients also differed between the two specimens.

(b) *Dynamic pressure*

For each step of protocol 1 we measured dynamic pressure on the ventral side of the tail at the root of the covert feathers (figure 1), at 1 mm intervals from the surface at an airspeed of 9.2 m s^{-1}; the depth at which dynamic pressure becomes positive is a measure of the depth of the separation bubble (figure 4*a*). We also determined the point at which the separation bubble reattached on the ventral surface of the tail. Following the first manipulation (01–02) there was little change in either the dynamic pressure profile through the boundary layer or in the 4 mm depth of the separation bubble. On removal of the ventral covert feathers (step 03), the separation bubble depth increased to 9 mm, and after complete removal of the tail (step 04) it further increased slightly to 11 mm. These patterns of increasing size of separation bubble confirm the hypothesis that the tail acts as a splitter plate and the covert feathers as a wedge to regulate vortex formation and separation. The dynamic pressure measurements showed that the remnants of the rectrices (03) still functioned to reduce the size of the separation bubble, even though it no longer reattaches. Splitter plates have an optimum size, above which no additional effect on the wake will be achieved, but additional drag due to the plate will be encountered, and below which increasing vorticity will be present in the wake, but will be controlled to a differing degree depending on plate size (Anderson & Szewczyk 1997).

We also measured dynamic pressure in the boundary layer on the dorsal and ventral sides of the centre point of the tail for steps 02 and 03 of protocol 2 (figure 4*b*). As might be expected, the gradient in dynamic pressure across the tail was much smaller after the centre portion of the tail had been removed; more surprisingly, the profile of dynamic pressure with height changed little. Removal of a centre portion of the rectrices enabled the boundary layers on either side of the body to interact, and eliminated the suction force that encourages the separation region to reattach to the ventral side of the tail. The reduced dynamic pressure in the dorsal region is responsible for broadening of the wake (see § 3c) and therefore for increasing drag; this is further confirmation that the furled tail acts as a splitter plate.

(c) *Flow visualization*

If the splitter plate model is valid, there should be changes to the dimensions of the wake (and vortex shedding characteristics of the body) between tail manipulations as the splitter plate and wedge are removed. Flow visualization during stages 01, 02 and 04 of protocol 2 (figure 5) shows that the position at which the flow separates from the ventral contour of the body and the

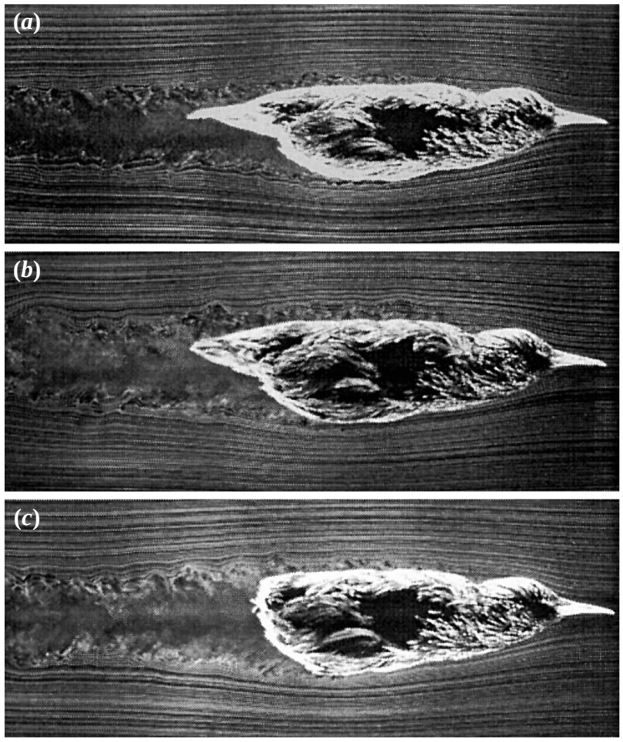

Figure 5. Flow visualization around the mounted, wingless body of a starling in a wind tunnel at 9 m s^{-1} (Reynolds number of 35 000) for steps 01, 02 and 04 of protocol 1 (*a*, *b* and *c* respectively). The position beyond which the streamlines cease to follow the ventral side contour of the body is similar for all three tail configurations. From *a* to *b* to *c* the height of the wake rises, but in *a*, and to some extent in *b*, the ventral separation bubble reattaches to the tail, as shown by dynamic pressure measurements (figure 4*a*). In each case the ventral boundary layer remains laminar until the deepest part of the body. The dorsal boundary layer becomes increasingly turbulent, even at these relatively low Reynolds numbers, as the tail is progressively removed; transition is triggered by a laminar separation bubble in the depression formed by the neck.

pattern of streamlines on the dorsal side remained similar for all treatments (although figure 5*b* shows increased turbulence in the dorsal boundary layer associated with laminar separation in the neck region; Maybury *et al.* 2001). The main difference was a significant increase in the mean height of the wake with treatment (figure 2), rising from 35.4 ± 2.3 mm for step 01 to 37.9 ± 1.4 mm for step 02 and 45.2 ± 2.1 mm for step 04 (ANOVA, $F_{2,15} = 39.5$, $p < 0.001$), corresponding to the measured increase in mean drag. This result also is consistent with the splitter plate/wedge hypothesis.

4. DISCUSSION

In steady flight a furled tail reduces body drag by the same mechanism as a combination of a splitter plate and a wedge. This mechanism is effective even though the bird's body lacks the symmetry of the objects on which splitter plates are normally applied. Removal or manipulation of the starling's rectrices enlarged the size of the separation bubble formed beneath the tail, increased wake height, and increased overall drag. Removal of the ventral covert feathers also had deleterious effects on separation bubble size and drag forces. The tail feathers themselves function as a splitter plate, encouraging reattachment of flow separated ventrally, while the covert feathers acts as a wedge; both manipulate the movement of vortices shed from the body, and make an important, and approximately equal, contribution to drag reduction.

These observations reveal that body drag is dominated by body–tail interactions. We removed the (large) lift and drag of the wings to isolate body drag, but in doing so we also eliminated both wing–body interference (which may also affect body drag; Gesser *et al.* 1998), and wing–tail interactions which have been shown to have a significant effect on wing and tail lift (Hummel 1992). The normal approach to bird aerodynamics has been to consider the bird as the sum of isolated body, wings and (sometimes) tail working independently of one another (see, for example, Pennycuick 1975; Thomas 1993, 1996*b*). Our experiments (see also Maybury *et al.* 2001) emphasize that this fragmented approach to bird aerodynamics is unrealistic, and that a bird should be explored theoretically and experimentally as an aerodynamic whole.

A bird's body lacks dorsoventral symmetry. The dorsal side of the body did not encounter the same problem of separation as the ventral side, as a consequence of the relatively smooth and more streamlined dorsal profile, and of the more dorsal location of the tail. Flow separates over the ventral surface of the bird in large part since the maximum girth is reached immediately anterior to the tail; because of morphological constraints arising from the location of the pelvis, the articulation of the hind legs, and the location of the viscera largely posterior to the flight muscles, the body narrows sharply beyond this point. Accordingly, those birds with relatively more slender bodies may be less prone to ventral separation; they may have less need for aerodynamic mechanisms to maintain flow, and might be expected to have smaller tails. The tail, when furled in steady flight, and the ventral covert feathers act as an aerodynamic counter measure to the otherwise deleterious effects of the avian Bauplan on body aerodynamics, and together reduce body drag by between 20 and 35% compared to that of a body of similar morphology but with no tail. We believe that this performance advantage—which is likely to be largely common to all birds—has been a major factor in the evolution of the avian tail (Rayner *et al.* 2001). This aerodynamic adaptation may have pre-adapted a relatively short tail for subsequent modification for flight control, as a subsidiary lifting surface, or as an organ for signalling in sexual selection.

W.J.M. was supported by a research studentship from Biotechnology and Biological Sciences Research Council (BBSRC). Experiments were funded by BBSRC research grant S03843 to J.M.V.R. The wind tunnel fan was provided by the London Fan Company. We thank Sally Ward for video films of starlings in flight, and Arthur Goldsmith for supplying the starling specimens.

REFERENCES

Anderson, E. A. & Szewczyk, A. A. 1997 Effects of a splitter plate on the near wake of a circular cylinder in 2 and 3-dimensional flow configurations. *Exp. Fluids* **23**, 161–174.

Barbosa, A. & Møller, A. P. 1999 Aerodynamic costs of long tails in male barn swallows *Hirundo rustica* and the evolution of sexual size dimorphism. *Behav. Ecol.* **10**, 128–135.

Batill, S. M. & Mueller, T. J. 1981 Visualization of transition in the flow over an airfoil using the smoke-wire technique. *AIAA J.* **19**, 340–345.

Bonser, R. H. C. & Rayner, J. M. V. 1996 Measuring leg thrust forces in the common starling. *J. Exp. Biol.* **199**, 435–439.

Buchanan, K. L. & Evans, M. R. 2000 The effect of tail streamer length on aerodynamic performance in the barn swallow. *Behav. Ecol.* **11**, 228–238.

Degani, D. 1991 Effect of splitter plate on unsteady flows around a body of revolution at incidence. *Phys. Fluids* A **3**, 2122–2131.

Denny, M. W. 1993 *Air and water. The biology and physics of life's media.* Princeton University Press.

Evans, M. R. & Thomas, A. L. R. 1997 Testing the functional significance of tail streamers. *Proc. R. Soc. Lond.* B **264**, 211–217.

Evans, M. R., Martins, T. L. F. & Haley, M. 1994 The asymmetrical cost of tail elongation in red-billed streamertails. *Proc. R. Soc. Lond.* B **256**, 97–103.

Fitzpatrick, S. 1997 Patterns of morphometric variation in birds' tails: length, shape and variability. *Biol. J. Linn. Soc.* **62**, 145–162.

Fitzpatrick, S. 1999 Tail length in birds in relation to tail shape, general flight ecology and sexual selection. *J. Evol. Biol.* **12**, 49–60.

Gatesy, S. M. & Dial, K. P. 1996 From frond to fan: *Archaeopteryx* and the evolution of short tailed birds. *Evolution* **50**, 2037–2048.

Gesser, R., Wedekind, F., Kockler, R. & Nachtigall, W. 1998 Aerodynamische Untersuchungen an naturnahen Starenmodellen. 2. Flügel-Rumpf Interferenzen. In *Biona report 13, Motion Systems* (ed. R. Blickhan, A. Wisser & W. Nachtigall), pp. 257–258. Jena, Germany: Gustav Fischer Verlag.

Hoerner, S. F. 1958 *Fluid-dynamic drag: practical information on aerodynamic and hydrodynamic resistance*, 2nd edn. New Jersey: author (private publication).

Von Holst, E. & Küchemann, D. 1941 Biologische und aerodynamische Probleme des Tierfluges. *Naturwissenschaften* **29**, 348–362. [Trans. Biological and aerodynamical problems of animal flight. *J. R. Aeronaut. Soc.* **46**, 39–56, 1942 (abridged) and *NASA Tech. Mem.* **75337**, 1980.]

Hummel, D. 1991 On the aerodynamics of the tail in birds. *Acta XX Congr. Int. Orn.* **2**, 730–736.

Hummel, D. 1992 Aerodynamic investigations on tail effects in birds. *Z. Flugwiss. Weltraumforsch.* **16**, 159–168.

Mansingh, V. & Oosthuizen, P. H. 1990 Effects of splitter plates on the wake flow behind a bluff body. *AIAA J.* **28**, 778–783.

Maybury, W. J. 2000 *The aerodynamics of bird bodies.* PhD thesis, University of Bristol, UK.

Maybury, W. J., Rayner, J. M. V. & Couldrick, L. B. 2001 Lift generation by the avian tail. *Proc. R. Soc. Lond.* B **268**. (In the press.)

Minitab Inc. 1995 *Minitab reference manual.* Release 10Xtra edition. Minitab Inc., PA, USA.

Møller, A. P., Barbosa, A., Cuervo, J. J., de Lope, F., Merino, S. & Saino, N. 1998 Sexual selection and tail streamers in the barn swallow. *Proc. R. Soc. Lond.* B **265**, 409–414.

Nakamura, Y. 1996 Vortex shedding from bluff bodies with splitter plates. *J. Fluids Struct.* **10**, 147–158.

Norberg, R. Å. 1994 Swallow tail streamer is a mechanical device for self-deflection of tail leading-edge, enhancing aerodynamic efficiency and flight manoeuvrability. *Proc. R. Soc. Lond.* B **257**, 227–233.

Norberg, U. M. 1990 *Vertebrate flight: mechanics, physiology, morphology, ecology and evolution.* Heidelberg, Germany: Springer.

Pennycuick, C. J. 1975 Mechanics of flight. In *Avian biology*, vol. 5 (ed. D. S. Farner, J. R. King & K. C. Parkes), pp. 1–73. New York: Academic Press.

Pennycuick, C. J., Obrecht, H. H. & Fuller, M. R. 1988 Empirical estimates of body drag in large waterfowl and raptors. *J. Exp. Biol.* **135**, 253–264.

Peters, D. S. & Gutmann, W. F. 1985 Constructional and functional preconditions for the transition to powered flight in vertebrates. In *The beginnings of birds* (ed. M. K. Hecht, J. H. Ostrom, G. Viohl & P. Wellnhofer), pp. 233–242. Eichstätt: JuraMuseum.

Rae, W. H. & Pope, A. 1984 *Low-speed wind tunnel testing*, 2nd edn. New York: Wiley-Interscience.

Rayner, J. M. V. 2001 On the origin and evolution of flapping flight aerodynamics in birds. In *New perspectives on the origin and early evolution of birds* (ed. J. Gauthier). *Spec. Publs Yale Peabody Mus.* (In the press.)

Rayner, J. M. V., Maybury, W. J. & Couldrick, L. B. 2001 Aerodynamic control by the avian tail. *Am Zool.* (Submitted.)

Thomas, A. L. R. 1993 On the aerodynamics of birds' tails. *Phil. Trans. R. Soc. Lond.* B **340**, 361–380.

Thomas, A. L. R. 1996*a* Why do birds have tails: the tail as a drag reducing flap, and trim control? *J. Theor. Biol.* **183**, 247–253.

Thomas, A. L. R. 1996*b* The flight of birds that have wings and a tail: variable geometry expands the envelope of flight performance. *J. Theor. Biol.* **183**, 237–245.

Tucker, V. A. 1990 Measuring aerodynamic interference drag between a bird body and the mounting strut of a drag balance. *J. Exp. Biol.* **154**, 439–461.

Ward, S., Rayner, J. M. V., Möller, U., Jackson, D. M., Nachtigall, W. & Speakman, J. R. 1999 Heat transfer from starlings *Sturnus vulgaris* during flight. *J. Exp. Biol.* **202**, 1589–1602.

Young, A. D. 1989 *Boundary layers.* Oxford, UK: Blackwell Scientific.